NUMERICAL INVESTIGATION OF THE STABILITY AND CONTROL OF SEPARATING BOUNDARY-LAYER FLOW

Matthieu Marquillie
Université de Nice-Sophia Antipolis
Laboratoire J.-A. Dieudonné
Parc Valrose; F-06108 Nice Cedex 2, France
marqui@math.unice.fr

Uwe Ehrenstein
Université de Nice-Sophia Antipolis
Laboratoire J.-A. Dieudonné
Parc Valrose; F-06108 Nice Cedex 2, France
uwe.ehrenstein@unice.fr

ABSTRACT

A boundary-layer flow along a bump is investigated numerically. At the rear of the bump the flow separates and the separation bubble becomes unstable above a critical Reynolds number. The resulting vortex shedding is reproduced numerically. Performing a local linear stability analysis of velocity profiles inside the separation bubble, it is shown that there is a relationship between a local absolute instability and the numerically observed global flow behaviour. First numerical experiments of flow control, reducing the recirculation length using blowing and suction, are performed as well.

INTRODUCTION

Laminar separating flow occurs in many engineering applications such as turbomachinery flow or in low-Reynolds number aerodynamics. Flow separation is synonymous with loss of performance such as increase in drag or for instance loss of lift on airfoils at angles of attack close to stall values.

Hence, the prediction (and prevention) of flow separation is a field of active research in fluid dynamics. Flow separation appears in the presence of adverse pressure gradients. One prototype geometry for separating flow is the backward facing step and for instance Kaiktsis *et al* (1996) have performed an exhaustive analysis of the stability of separation bubbles for this flow geometry. One has to make a distinction between geometry induced separation, and separation on smooth surfaces induced by adverse pressure gradients. In the numerical investigations of Pauley *et al.* (1994), among others, an adverse pressure gradient is produced by suction through the upper boundary. In recent experiments on laminar separation bubbles (Häggmark *et al* (2001)), the adverse pressure gradient is imposed on the boundary-layer flow along the plate by an opposite contoured wall with suction.

In the present investigation separating flow is induced by a smooth bump mounted on a flat plate. The flow transits continuously from a favourable to an adverse pressure gradient leading to separation at the rear of the bump. Note that the geometry of the bump has originally been designed for turbulent flow measurements (Bernard *et al* (2001)). We briefly summarize in the next Section the numerical solution procedure used to accurately describe the separating steady and unsteady flow. It is then shown that above a critical Reynolds number self-sustained vortex shedding occurs. For the steady state just below the critical global Reynolds number the streamwise velocity profiles are analysed with respect to the local linear stability behaviour. It is shown that there is a transition from local convective to local linear absolute instability, which lends some credit to the idea that the global unsteady and nonlinear behaviour is triggered by a local (linear) absolute instability. Finally, we apply a instantaneous suboptimal control strategy (Choi *et al* (1999)) to illustrate the possibility of reducing the length of the recirculation zone by blowing and suction at the summit of the bump.

GEOMETRY AND NUMERICAL SOLUTION PROCEDURE

The two-dimensional Navier-Stokes system is made dimensionless using the displacement thickness at inflow as reference length, the flow velocity at infinity being the reference velocity. The flow domain is $x_a^* \leq x^* \leq x_b^*$, $\eta^*(x^*) \leq y^* < \infty$, with $\eta^*(x^*)$ the lower boundary containing the bump (cf. Figure 1). The flow geometry is transformed into a Cartesian one using the mapping

$$t = \bar{t}\,,\; x = \bar{x}\,,\; y = \bar{y} - \bar{\eta}(\bar{x}). \qquad (1)$$

(the barred coordinates being the physical ones). The gradient, Laplacian and the curl operator now write

$$\bar{\vec{\nabla}} = \vec{\nabla} + \vec{G}_\eta,\; \bar{\Delta} = \Delta + L_\eta$$
$$\bar{\vec{\nabla}} \times (\bar{\vec{\nabla}} \times \vec{u}) = \vec{\nabla} \times (\vec{\nabla} \times \vec{u}) + \vec{R}_\eta(\vec{u}) \qquad (2)$$

with

$$\vec{G}_\eta = (-\frac{\partial \eta}{\partial x}\frac{\partial}{\partial y}, 0),$$
$$L_\eta = -\frac{\partial^2 \eta}{\partial x^2}\frac{\partial}{\partial y} - 2\frac{\partial \eta}{\partial x}\frac{\partial^2}{\partial x \partial y} + (\frac{\partial \eta}{\partial x})^2 \frac{\partial^2}{\partial y^2},$$
$$\vec{R}_\eta(\vec{u}) = (-\frac{\partial \eta}{\partial x}\frac{\partial^2 v}{\partial y^2}, -\frac{\partial \eta}{\partial x}\frac{\partial^2 u}{\partial y^2} - L_\eta v). \qquad (3)$$

The system to be solved in the computational coordinates (x, y) is

$$\frac{\partial \vec{u}}{\partial t} + (\vec{u}.\vec{\nabla})\vec{u} + (\vec{u}.\vec{G}_\eta)\vec{u}$$
$$= -\vec{\nabla} p - \vec{G}_\eta p + \frac{1}{Re}\Delta \vec{u} + \frac{1}{Re} L_\eta \vec{u} \qquad (4)$$

$$\vec{\nabla}.\vec{u} = -\vec{G}_\eta.\vec{u} \qquad (5)$$

in the transformed geometry $x_a \leq x \leq x_b$, $0 \leq y < \infty$ (in the wall-normal y direction an algebraic mapping transforms the unbounded domain into a finite one). Fourth-order finite differences are used in the streamwise x-direction whereas the wall-normal direction is discretized using Chebyshev-collocation. Second-order backward Euler differencing is used in time: the Cartesian part of the diffusion term is taken implicitly whereas the nonlinear and metric terms are evaluated using an explicit second-order Adams-Bashforth scheme. In order to ensure a divergence free velocity field a fractional time-step procedure is used (Marquillie and Ehrenstein (2001)). At inflow, a Blasius profil is prescribed whereas at outflow we use the advection condition

$$\frac{\partial \vec{u}}{\partial t} + U_c \frac{\partial \vec{u}}{\partial x} = 0,$$
$$U_c = \frac{1}{y^*}\int_0^{y^*} u(x_b, y)dy, \qquad (6)$$

which proved to be appropriate to evacuate the vortex structures without reflection for convenient convection velocities U_c.

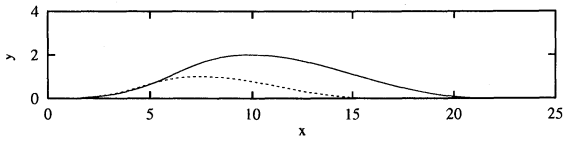

Figure 1: Geometry of the bump; ——: $h = 2$, aspect ratio $L_c/h = 10$.

RESULTS

In all the forthcoming simulation results a bump with height $h = 2$ has been considered, for a aspect ratio (length versus height) of 10. The streamwise direction (of length 200) has been discretized using a grid with 1000 points whereas 92 collocation points have been considered in the wall-normal direction.

Global computations

The flow is characterized by a separation bubble at the rear of the bump the size of which increasing with the inflow Reynolds number (Marquillie and Ehrenstein (2001)). One steady state for an inflow Reynolds number of $Re = 600$ is shown in Figure 2 (note that the Reynolds number based on the bump height $h = 2$ is $Re = 1200$). Our numerical experiments have shown that this Reynolds number is nearby criticality. Indeed, increasing the Reynolds number to 650 the flow becomes definitely unstable (without injecting any controlled perturbation) as can be seen in Figure 3, where successive instantaneous streamlines are shown exhibiting vortex shedding. The vortex-shedding hence results from a self-induced instability mechanism and one may wonder whether there is a connection with a local linear absolute instability behaviour.

Local linear stability analysis

Extracting the local streamwise velocity profiles $U(y)$ from the last stable state we have recovered at $Re = 600$, a conventional linear stability analysis for the parallel flow $(U(y), 0)$ using normal modes

$$\vec{u} = (\hat{u}(y), \hat{v}(y))\; e^{i(\alpha x - \omega t)},$$

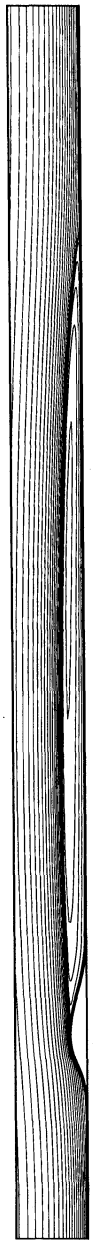

Figure 2: Instantaneous streamlines, $0 \leq x \leq 150$, for the steady state at $Re = 600$.

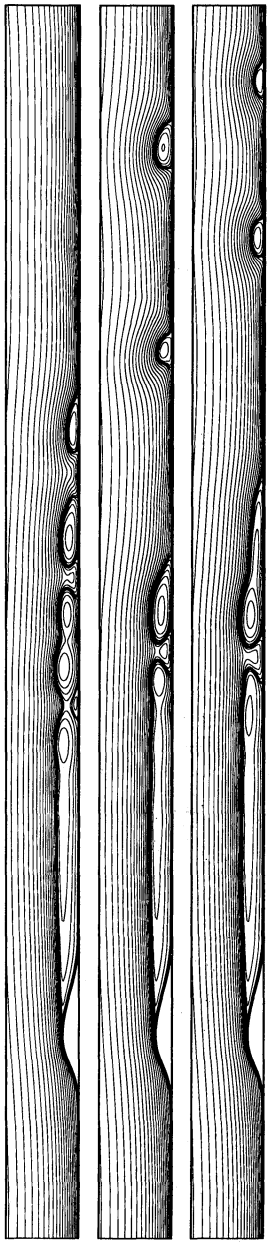

Figure 3: Successive instantaneous streamlines, unsteady flow at $Re = 650$.

$$p = \hat{p}(y)\ e^{i(\alpha x - \omega t)}, \eta = \hat{\eta}\ e^{i(\alpha x - \omega t)}, \qquad (7)$$

has been performed, solving numerically the eigenvalue problem for the dispersion relation $D(\omega, \alpha) = 0$. A spatio-temporal analysis has been performed determining alternatively $\omega(\alpha)$ as well as $\alpha(\omega)$ for both complex wavenumbers α and frequencies ω. Computing the spatial branches for the Laplace contours $\omega_i = cte$ (with $\omega = \omega_r + i\omega_i$), absolute instability occurs if two branches $\alpha^+(\omega), \alpha^-(\omega)$ (initially located at opposite sides of the real axis in the complex wavenumber plane) coalesce for $\omega_i > 0$, when lowering the Laplace contour. At the point of coalescence $D(\alpha_0, \omega_0) = 0, \frac{\partial D}{\partial \alpha}(\alpha_0, \omega_0) = 0$ or equivalently $\frac{\partial \omega}{\partial \alpha}(\alpha_0) = 0$ (Huerre et Monkewitz, (1990)).

For a locally absolutely unstable flow one would hardly be capable of retrieving a steady state for the global flow by numerical simulation. Analysing the flow profiles (for the last steady state at $Re = 600$) inside the recirculation bubble for different x-locations, it appears that the profile at $x = 35$ (the summit of the bump being located at $x = 25$) is that for which pinching occurs for a Laplace contour the closest to the real axis (though still for $\omega_i < 0$). The pinching process for the spatial branches is shown in Figure 4. Comparing profiles at $Re = 550$ with the corresponding profile

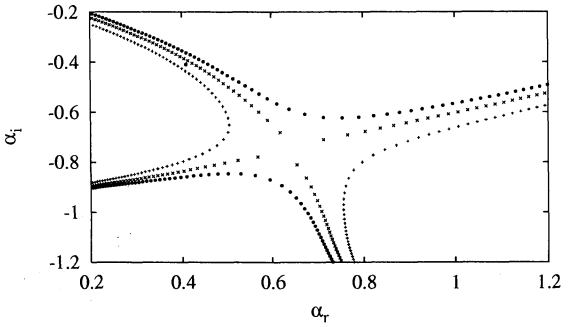

Figure 4: Laplace contours $\omega_i = cte$ in the plane (α_r, α_i), in the vicinity of the pinch point: oo : $\omega_i = -0.03$; $\times\times$: $\omega_i = -0.038$; ++ : $\omega_i = -0.05$.

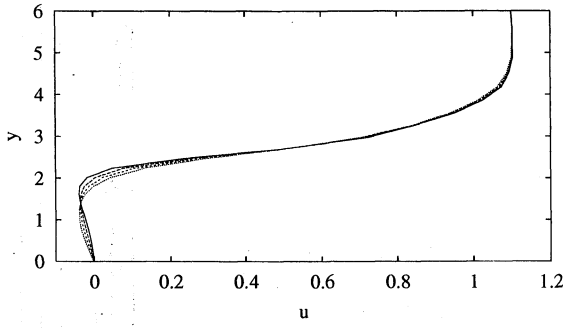

Figure 5: Profiles $U(y)$ extrapolated from profile at $Re = 600$: $\cdots$, to: — absolutely unstable profile.

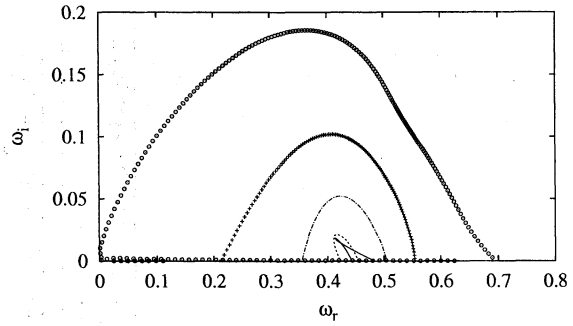

Figure 6: $\alpha_i = cte$ contours in the plane (ω_r, ω_i) : oo : $\alpha_i = 0$; + + + : $\alpha_i = -0.5$; $- \cdot -$: $\alpha_i = -0.7$; $\cdots$ $\alpha_i = -0.8$; —· : $\alpha_i = -0.88$ (cusp).

at $Re = 600$, a simple extrapolation process (by adding the difference) has been performed leading to a profile which is indeed absolutely unstable, depicted as the solid line in Figure 5. Indeed, the $\alpha_i = cte$ - contours in the complex frequency plane shown in Figure 6 exhibit a cusp at $\alpha_i = -0.88$, that is at that point $\partial\omega/\partial\alpha = 0$ which is the condition for absolute instability. Note that the corresponding velocity profile is close to the profile coming out of the numerical simulation inside the recirculation bubble at $Re = 600$, depicted as the dotted line in Figure 5. The reverse flow does not exceed 5 per cent put extends up to a height of $y = 2$.

Instantaneous control strategy by blowing-suction

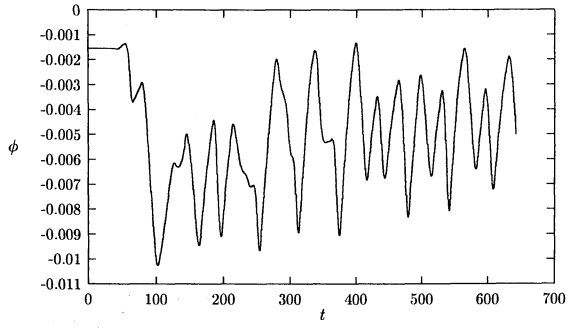

Figure 7: Time history of the blowing-suction amplitude ϕ for the controlled flow at $Re = 500$.

In a first attempt to apply optimal control strategy to the flow under consideration, we apply blowing-suction at the summit of the bump via the boundary condition $\vec{u}_{|\Gamma_c} = \vec{\Psi}$. For this purpose we use the methodology based on the Lagrangian functional (see Choi *et al* (1999) for a recent application to separating flow control), that is we solve the adjoint system

$$-\frac{\partial \vec{v}}{\partial t} + (\vec{\nabla}\vec{u})^T\vec{v} - (\vec{u}.\vec{\nabla})\vec{v} - \vec{\nabla}\pi - \frac{1}{Re}\Delta\vec{v} = 0 \qquad (8)$$

$$\vec{\nabla}.\vec{v} = 0 \qquad (9)$$

($\vec{v}$ being the adjoint velocity field and π the adjoint pressure) together with the Navier-Stokes equations. Here we prescribe the local blowing-suction profile (a polynomial graph ensuring net mass at the boundary), the amplitude Φ being the unknown. The objective function to minimize is $F(\vec{u}) = \int_{\Gamma_s}\left(\frac{\partial u}{\partial y}\left(\frac{\partial u}{\partial y} - \left|\frac{\partial u}{\partial y}\right|\right)\right) ds$ (in order to locate the reattachment point in the vicinity of Γ_s). As an example we consider a steady state at $Re = 500$, the recirculation length in that case being 80. For this first numerical experiment we attempt to locate the reattachment point for the recirculation length to be 30. Instantaneous control strategy has been applied: for a given blowing-suction, the Navier-Stokes system is advanced one time-step, the adjoint system is computed backward and a new amplitude of blowing-suction is computed performing one gradient step $\Phi^{k+1} = \Phi^k - \alpha\nabla J(\Phi^k)$, J being the functional to minimize (containing the objective and the cost of blowing-suction). The resulting amplitude is shown in Figure 7: due to the instantaneous control procedure, using a constant α-value in the gradient algorithm, the blowing-suction amplitude oscillates

almost periodically. The corresponding instantaneous streamlines are depicted in Figure 8. The recirculation bubble is indeed reduced but due to the oscillatory blowing-suction unsteady (but more organized than in the uncontrolled case) vortex shedding occurs.

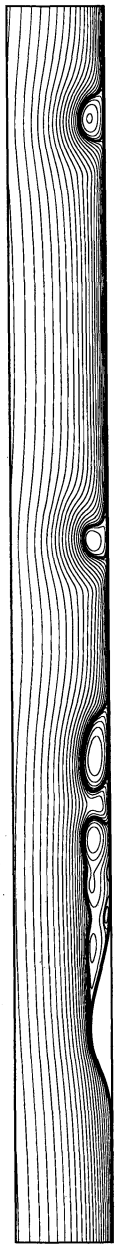

Figure 8: Instantaneous streamlines of the flow at $Re = 500$, in the domain $5 \leq x \leq 120$ for the controlled case.

CONCLUDING REMARKS

Recent investigations have been concerned with the construction of profiles characterizing separating boundary-layer flow (Hammond and Redekopp (1998), Alam and Sandham (2000)), focusing on a possible absolute instability behaviour. The present investigation reinforces the idea that indeed local, linearly absolutely unstable profiles are present in marginally unstable separating boundary layers and that the local instability behaviour is responsable for the global instability. One may expect that optimal control strategies could be applied to prevent the global instability or at least to organize the time-dependent flow.

REFERENCES

Alam, M. and Sandham, N.D., 2000, "Direct numerical simulation of 'short' laminar separation bubbles with turbulent reattachment", *J. Fluid Mech.*, **410**, pp. 1–28.

Bernard, A., Foucaut, J.M., Dupont, P. and Stanislas, M., 2001, "Control of a decelerating boundary–layer with the help of passive vortex generators", submitted to *AIAA Journal.*

Choi H., Hinze M., Kunisch k., 1999, "Instantaneous control of backward-facing step flows", *Appl. Num Math.*,**31**, pp. 133-158.

Häggmark, C.P., Bakchinov, A.A., Alfredsson, P.H., 2000, "Experiments on a two-dimensional laminar separation bubble", *Phil. Trans. R. Soc. London A*, **358**, pp. 3193-3205.

Hammond, D.A. and Redekopp, L.G., 1998, "Local and global instability properties of separation bubbles", *Eur. J. Mech. B–Fluids*, **17**, n° 2, pp. 145–164.

Huerre, P. and Monkewitz, P.A., 1990, "Local and global instabilities in spatially developping flows", *Ann. Rev. Fluid Mech.*, **22**, pp. 473–537.

Kaiktsis, L., Karniadakis, G.E. and Orszag, S.A., 1996, "Unsteadiness and convective instabilities in two–dimensional flow over a backward–facing step", *J. Fluid Mech.*, **321**, pp. 157–187.

Marquillie, M. and Ehrenstein, U., 2001, "Numerical simulation of separating boundary-layer flow", *Computers and Fluids*, to appear.

Pauley, L.L., 1994, "Structure of local pressure–driven three–dimensional transient boundary–layer separation", *AIAA Journal*, **32**, n° 5, pp. 997–1005.